

High-Pressure Transformations and Stability of Ferromagnesite in the Earth's Mantle

Eglantine Boulard, François Guyot, and Guillaume Fiquet

ABSTRACT

Ferromagnesite (Mg,FeCO_3) plays a key role in the transport and storage of carbon in the deep Earth. Experimental and theoretical studies demonstrated its high stability at high pressure and temperature against melting or decomposition. Several pressure-induced transformations of ferromagnesite have been reported at conditions corresponding to depths greater than ~ 1030 km in the Earth's lower mantle. Although there is still no consensus on their exact crystallographic structures, evidence is strong for a change in carbon environment from the low-pressure planar CO_3^{2-} ion into carbon atoms tetrahedrally coordinated by four oxygens. High-pressure iron-bearing phases concentrate a large amount of Fe^{3+} as a result of intra-crystalline self-redox reactions. These crystallographic particularities may have significant implications on carbon reservoirs and fluxes in the deep Earth.

11.1. INTRODUCTION

Carbon exchange between the Earth's interior and its surface occurs over time scales of hundreds millions of years, constituting the geodynamical carbon cycle. Superficial carbon is recycled into the deep earth by means of subduction. Estimations of this carbon influx ranges from 0.0001 to 52 megatons of carbon annually (Kelemen & Manning, 2015). This huge uncertainty hinges on poor constraints on the amount of carbon retained by subducting slabs. Carbonate inclusions in diamonds suggest that carbon is transported down to the transition zone depths (Brenker et al., 2007; Kaminsky, 2012; Wang et al., 1996); however, whether any carbon reaches the lower mantle is still controversial. Most subducted carbon is expected to melt and/or break down and return to the Earth's surface via volcanism (Kelemen & Manning, 2015; Thomson et al., 2016). However, relatively oxidizing conditions and low slab temperatures

may result in the transportation of carbon to greater depths that could feed the core-mantle boundary (CMB) (Martirosyan et al., 2015). Yet, a quantitative estimation of carbon or CO_2 released at the CMB remains unconstrained, as are precise mechanisms for transportation of volatiles to the very deep mantle. In particular, the behaviors of such phases in the presence of deep mantle minerals such as silicates, iron oxides, or metallic iron remain to be evaluated.

Carbon is recycled into the deep mantle chiefly as carbonates, which mainly occur as calcite CaCO_3 , dolomite $\text{CaMg}(\text{CO}_3)_2$, and magnesite MgCO_3 at the Earth's surface. Due to chemical reactions with silicates such as pyroxenes and bridgmanite, ferromagnesite (Mg-FeCO_3) is considered the dominant carbonate phase in the deep mantle (e.g. Biellmann et al., 1993; Kushiro et al., 1975; Wood et al., 1996). The behavior of ferromagnesite at depth is therefore critical for evaluating the storage capacity and fluxes of carbon. Because of the scarcity of natural samples coming from the lower mantle (e.g. Brenker et al., 2007; Kaminsky, 2012), knowledge of ferromagnesite's stability and behavior at depth mainly results from theoretical and experimental studies. The latter requires the ability to reach high pressure and

Sorbonne Université, UMR CNRS 7590, Muséum National d'Histoire Naturelle, IRD, Institut de Minéralogie, Physique des Matériaux et Cosmochimie-IMPMC, Paris, France

temperature (P-T) conditions of the Earth's mantle and to use microscale and nanoscale probes to characterize samples. Laser-heated diamond anvil cell is the main static pressure device for studying carbon-bearing phases at the Earth's mantle and core conditions. This technique permits the attainment of pressures above 300 GPa and temperatures up to 5000 K (Tateno et al., 2010) by heating with double-sided high-powered infrared lasers available in house and at synchrotron X-ray beamlines. The excellent transparency of single-crystal diamond to a wide range of electromagnetic radiation is compatible with numerous analytical probes for more comprehensive in situ characterization of high P-T behavior. This is critical in the case of nonquenchable phases or dynamic studies where “squeeze, cook, and look” experiments are not sufficient. A detailed review of the different techniques can be found in Mao and Boulard (2013).

In this chapter, we present a review of recent studies dealing with the high-pressure behavior of carbonates on the solid solution joining magnesite and siderite (FeCO_3). We first present ferromagnesite high-pressure behaviors

and structures. We then discuss evidence of particular processes such as the self-redox reactions of Fe-bearing carbonates. Finally, we discuss potential implications for the Earth's system.

11.2. COMPRESSION OF MG-Fe RHOMBOHEDRAL CARBONATE

Siderite and magnesite are isomorphous with calcite and crystallize in rhombohedral symmetry with the R-3c space group (Graf, 1961) (Figure 11.1a). Represented with a hexagonal unit cell, these carbonates contain six formula units per unit cell. They consist of an alternation of layers along the c-axis of cations (Fe^{2+} , Mg^{2+}) in six-fold oxygen coordination and carbon in trigonal planar (CO_3)²⁻ groups. The orientations of two consecutive carbonate ions are staggered relative to each other with the cation at the center of symmetry.

In situ X-ray diffraction (XRD) studies at high pressure show a high stability of rhombohedral MgCO_3 up to ~80 GPa–2500 K (Fiquet et al., 2002). No evidence of

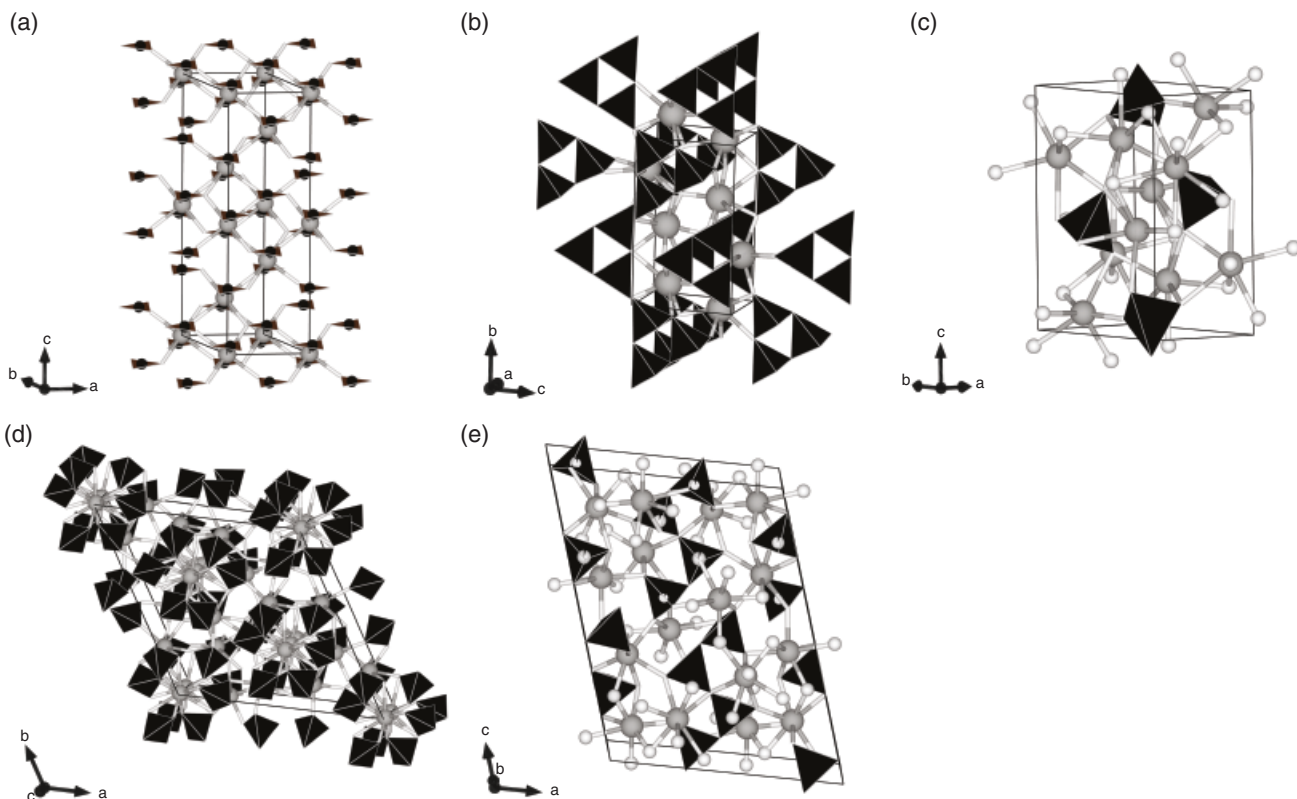


Figure 11.1 Crystallographic structures of Mg-Fe carbonates as reported in the literature. (a) The calcite-type rhombohedral structure in which Mg-Fe carbonates crystallize at ambient conditions, (b) high-pressure structure of magnesite and ferromagnesite (MgCO_3 and $\text{Mg}_{0.25}\text{Fe}_{0.31}[\text{C}_3\text{O}_9]_{0.233}$) (Boulard et al., 2011), (c) high-pressure phase of siderite: $\text{Fe}_4\text{C}_3\text{O}_{12}$ (Boulard et al., 2012), (d) $\text{Fe}_4\text{C}_3\text{O}_{12}$ (Cerantola et al., 2017), (e) $\text{Fe}_4\text{C}_4\text{O}_{13'}$ and $\text{Mg}_2\text{Fe}_2(\text{C}_4\text{O}_{13})$ (Cerantola et al., 2017; Merlini et al., 2015). White and grey spheres are oxygens and Fe/Mg cations respectively, and black triangle or black tetrahedra are carbon polyhedra. See electronic version for color representation of the figures in this book.

decomposition or melting under P-T conditions down to the CMB is observed (Dorogokupets, 2007; Fiquet et al., 2002; Gillet, 1993; Solopova et al., 2015). MgCO_3 can also be synthesized from the recombination of oxides MgO and CO_2 at mantle P-T conditions (Boulard et al., 2012; Scott et al., 2013). The c-axis is significantly more compressible than the a-axis, attributable to the tight bonding of C-O in CO_3 groups (Katsura et al., 1991). However, in situ XRD refinements and infrared (IR) spectroscopic analyses showed that from 20 to 50 GPa, C-O bonds lengthen before contracting (Fiquet et al., 2002; Santillán et al., 2005). This particular behavior, produced by the rotation of MgO_6 octahedra, likely contributes to the remarkable stability of the R-3c structure in carbonates at high pressure (Fiquet et al., 2002; Santillán et al., 2005).

The substitution of Fe^{2+} for Mg^{2+} increases the compressibility of ferromagnesite due to the Fe-O bond's length (2.141 Å) being longer than that of Mg-O (2.097 Å) (Liang et al., 2018). FeCO_3 and MgCO_3 present bulk moduli of 97 GPa and 103 GPa, respectively (Liang et al., 2018; J. Zhang et al., 1998). C-O bond length monotonically decreases upon compression up to ~40–45 GPa (Lavina et al., 2010; Santillán & Williams, 2004), the pressure at which Fe in ferromagnesite undergoes a spin transition (Liu et al., 2014; Mattila et al., 2007). It results in a lengthening of C-O bonds due to the shrinkage of Fe-O bonds, and an increase in density and incompressibility (Cerantola et al., 2015; Lavina et al., 2010; Lin et al., 2012). The Fe spin transition is expected to affect the partition coefficient of Fe between $(\text{Mg,Fe})\text{CO}_3$ and $(\text{Mg,Fe})\text{SiO}_3$ (Lobanov et al., 2015; Weis et al., 2017), leading to carbonate composition in equilibrium with Mg-Fe bridgmanite closer to siderite above 40–45 GPa.

Compared to magnesite, siderite decomposes at lower temperatures (~500° lower at 2 GPa) (Tao et al., 2013). Although the decarbonation boundary of siderite is very close to the average mantle geotherm at about 3 GPa (Tao et al., 2013), typical cold and hot subduction paths are well within the stability fields of both siderite and magnesite (Syracuse et al., 2010).

11.3. HIGH-PRESSURE POLYMORPHISM OF FERROMAGNESITE

High P-T phase transition in MgCO_3 was first demonstrated experimentally by Isshiki et al. (2004) who observed diffraction peaks at 115 GPa–2200 K that could not be assigned to any decomposition products (MgO or CO_2). Transmission electron microscopy analyses on the recovered sample showed a homogeneous amorphous sample area rich in Mg, C, and O (Irifune et al., 2005). This discovery inspired significant interest in both experimental and theoretical mineral physics. Systematic searches through databases of known crystal structures

combined with energy minimization first indicated that a pyroxene structure (space group C2/c) becomes energetically more favorable than magnesite above ~100 GPa (Skorodumova, 2005). Later, Oganov et al. (2006) reported that a C22₁ pyroxene-type structure, also predicted in CaCO_3 , was even more stable. Both structures contain zigzag chains of corner-sharing CO_4^{4-} tetrahedra.

Pressure-temperature conditions at which experimental studies reported phase transitions of ferromagnesite are reported in Figure 11.2. There is no consensus about those high-pressure crystallographic structures (Figure 11.1 and Table 11.1) (Boulard et al., 2011, 2012; Cerantola et al., 2017; Isshiki et al., 2004; Liu et al., 2015; Merlini et al., 2015). Those differences might be due to the existence of multiple low-enthalpy structures (metastable) that are competitive over a wide pressure range (Oganov et al., 2008) and/or to differences in compositions of the starting material.

Concerning the magnesian end-member, Isshiki et al. (2004) proposed an orthorhombic structure above 115 GPa–2200 K (noted Mag-II in Figure 11.2). No atom positions were proposed because no structural refinement could be performed. In 2011, Boulard et al. reported a transition of magnesite into a monoclinic structure above 80 GPa at 2300 K. Rietveld refinement was not possible, but through comparison with theoretical studies (Oganov et al., 2008), a crystalline structure with a P2₁/c space group made of groups of three $(\text{CO}_4)^{4-}$ tetrahedra sharing one corner that constitute $(\text{C}_3\text{O}_9)^{6-}$ rings, was proposed (Figure 11.1b). Mg-Fe composition was refined with the same structure (Fe-Mag-II). Nonhydrostatic conditions might have favored metastable phases in those experiments as no pressure medium was used. However, reversal reactions using oxides as starting materials (e.g. $\text{MgO} + \text{CO}_2$) to maximize synthesis of thermodynamically stable phases yielded same structure.

From recombination of FeO and CO_2 oxides, Boulard et al. (2012) show that rhombohedral siderite coexists with a new structure (Sid-II) from ~40 GPa–1400 K (Figure 11.1c) to ~70 GPa–2200 K, above which siderite fully disappears. The chemical composition, $\text{Fe}_4\text{C}_3\text{O}_{12}$, was deduced from electron energy-loss spectroscopy (EELS) analyses on the recovered samples following the method developed by Egerton (1996). Due to the similarity in chemical composition and unit cell parameters with the olivine-structured Laihunite silicate $(\text{Fe}^{3+}, \text{Fe}^{2+})_2\text{SiO}_4$, Boulard et al. (2012) proposed a monoclinic structure (P2₁/b space-group) based on isolated $(\text{CO}_4)^{4-}$ groups.

A single high-pressure phase, Sid-II/Fe-Mag-II, with an orthorhombic unit cell was proposed by Liu et al. (2015). It is still unclear whether this structure is based on CO_4 groups. More recently, single crystal XRD studies were performed on $(\text{Mg,Fe})\text{CO}_3$ (Merlini et al., 2015) and FeCO_3 (Cerantola et al., 2017), allowing

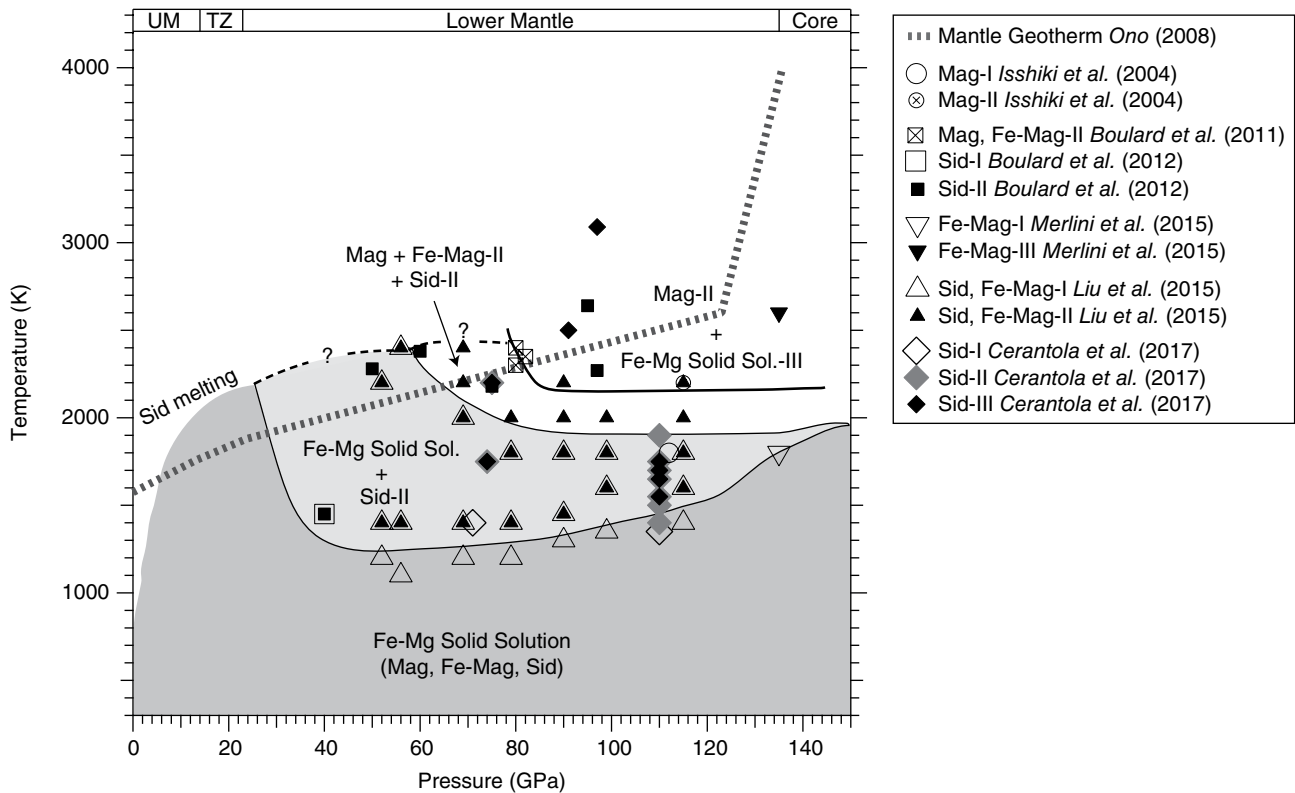


Figure 11.2 Experimental ferromagnesite phase diagram. Mag-I, Sid-I, and Fe-Mag-I refer to ambient magnesite, siderite, and ferromagnesite structures; phases II and III to the associated high-pressure polymorphs. See electronic version for color representation of the figures in this book.

structural refinements of crystallographic structures with atom position determinations. At pressure above 74 GPa and temperature between 1400 K and 1650 K, Cerantola et al. (2017) observed transformation of FeCO₃ into an Fe₄C₃O₁₂ high-pressure phase (Sid-II), an hexagonal structure with R-3c space group formed by isolated CO₄ groups. They used the same hexagonal cell to fit the diffraction pattern from Liu et al. (2015). Up to 2500 K, Fe₄C₃O₁₂ coexists with a second high-pressure phase, Fe₄C₄O₁₃ (Sid-III), a monoclinic structure with zigzag-shaped (C₄O₁₃)¹⁰⁻ chains formed by four corner-shared CO₄ groups, a phase previously described by Merlini et al. (2015) for ferromagnesite at 135 GPa–2600 K (2900 km).

11.3.1. Evidence for Tetrahedrally Coordinated Carbon

Identification of CO₄ groups in high-pressure structures based solely on XRD is difficult as it requires precise structural refinements. Moreover, localizing light elements such as carbon is not easy. Only Merlini et al. (2015) and Cerantola et al. (2017) could demonstrate tetrahedrally coordinated carbon from direct single-crystal-XRD measurements in the stoichiometries: Mg₂Fe₂C₄O₁₃, Fe₄C₄O₁₃, and Fe₄C₃O₁₂.

Vibrational spectroscopies, Raman and IR, are also particularly sensitive to carbon chemical environment and directly probe C-O bonds. Boulard et al. (2015) reported the first in situ characterization of C-O bonds in Fe-Mag-II. They found that its IR spectrum exhibits unique features not present in the low-pressure spectrum. The band assignment relied on first-principles calculations of the IR spectrum of tetrahedrally coordinated carbon in MgCO₃ (P2₁/a space group). A mode at ~1,304 cm⁻¹ at ~80 GPa, characteristic of the C-O asymmetric stretching vibration in CO₄ groups, could be used as a fingerprint of CO₄ groups in high-pressure mineral phases. An intense Raman band at ~1,025 cm⁻¹ (at 105 GPa) with a pressure dependence of ~1.8 cm⁻¹/GPa in P2₁/c CaCO₃ was recently proposed as characteristic of the symmetrical stretching vibration in its CO₄ groups (Lobanov et al., 2017).

While the high-pressure structures amorphized upon decompression, electron and X-ray spectroscopies at the carbon K-edge performed on recovered samples show that they preserved spectroscopic signatures in the amorphous phase, which could be associated to carbon-oxygen tetrahedral polyhedral. Analyses were either collected by EELS using transmission electron microscopy or by synchrotron radiation-based scanning transmission X-ray

Table 11.1 Crystallographic structures of high-pressure Mg-Fe carbonate polymorphs from experimental studies.

Composition	Theoretical Calculations	P Range (GPa)	Space Group	a	b	c	β
MgCO₃	Skorodumova et al., 2005	>113	C2/c				
	Oganov et al., 2006	>107	C222 ₁	5.552	7.201	2.880	
	Oganov et al., 2008	82–138	C2/m	8.094	6.488	6.879	103.98
		138–160	P2 ₁	4.534	7.792	5.086	104.54
	Experimental Studies						
	Starting Material						
MgCO₃	Isshiki et al., 2004	>115	Ortho.	7.18	5.03	4.47	
	Mg _{0.994} Ca _{0.006} CO ₃						
Mg₂Fe₂(C₄O₁₃)	Boulard et al., 2011	>80	P21/c	8.37	6.37	6.80	104.57
	Mg _{0.997} Fe _{0.003} CO ₃						
Mg_{0.25}Fe_{0.3}(C₃O₉)_{0.233}	Merlini et al., 2015	135	Mono.	9.822	3.902	13.154	108.02
	Mg _{0.26} Fe _{0.7} Mn _{0.025} Ca _{0.015} CO ₃						
Fe₄C₄O₁₃	Boulard et al., 2011	>80	P21/c	7.83	6.37	6.73	101.97
	Mg _{0.249} Fe _{0.748} Mn _{0.005} Ca _{0.006} CO ₃						
Fe₄C₃O₁₂	Cerantola et al., 2017	>74	C12/c1	10.261	3.985	13.455	107.85
	FeCO ₃						
Fe₄C₃O₁₂	Cerantola et al., 2017	>74	R3c	12.762	12.762	5.332	
	FeCO ₃						
FeCO₃	Boulard et al., 2012 FeO+CO ₂	>50	Mono.	10.16	6.66	6.15	93.04
	Liu et al., 2015	>50	Pmm2	10.99	6.34	5.27	
	Fe _{0.998} Mn _{0.002} CO ₃						
	Mg _{0.33} Fe _{0.65} Mn _{0.2} CO ₃						

Table 11.2 Self-oxidation reactions experimentally observed.

Reaction #	Reference	Chemical Reaction
R1	Merlini et al., 2015	$93\text{Fe}_{0.7}\text{Mg}_{0.3}\text{CO}_3 = 20\text{Mg}_{1.395}\text{Fe}_{2.605}(\text{C}_4\text{O}_{13}) + \text{Fe}_{13}\text{O}_{19} + 13\text{C}$
R2	Boulard et al., 2011	$20\text{Mg}_{0.25}\text{Fe}_{0.75}\text{CO}_3 = 20\text{Mg}_{0.25}\text{Fe}_{0.3}(\text{C}_3\text{O}_9)_{0.233} + 3\text{Fe}_3\text{O}_4 + 6\text{CO}$ (or $3\text{C} + \text{CO}_2$)
R3	Boulard et al., 2012	$4\text{FeO} + 4\text{CO}_2 \rightarrow \text{Fe}_4\text{C}_3\text{O}_{12} + \text{C}$
R4	Boulard et al., 2012	$4\text{FeO} + 5\text{CO}_2 = \text{Fe}_4\text{C}_3\text{O}_{12} + 2\text{CO}$
R5	Boulard et al., 2012	$2\text{Fe}_2\text{O}_3 + 3\text{CO}_2 = \text{Fe}_4\text{C}_3\text{O}_{12}$
R6	Cerantola et al., 2017	$4\text{FeCO}_3 = \text{Fe}_4\text{C}_3\text{O}_{12} + \text{C}$
R7	Cerantola et al., 2017	$7\text{Fe}_4\text{C}_3\text{O}_{12} + 3\text{C} = 6\text{Fe}_4\text{C}_4\text{O}_{13} + 2\text{Fe}_2\text{O}_3$
R8	Cerantola et al., 2017	$8\text{Fe}_4\text{C}_3\text{O}_{12} = 6\text{Fe}_4\text{C}_4\text{O}_{13} + 4\text{Fe}_2\text{O}_3 + 3\text{O}_2$

microscopy coupled to the acquisition of X-ray absorption spectra. C K-edge on an ambient pressure rhombohedral (R-3c) carbonate sample display peaks at 290.3 and 298.3 eV assigned to $1s \rightarrow p^*$ electronic transition and one peak at 300.5 eV assigned to $1s \rightarrow s^*$, within carbonate CO_3 groups (Hofer & Golob, 1987; Zhou et al., 2008). Spectra collected on recovered samples transformed into the high-pressure phases of the two compositions FeCO_3 and $(\text{Mg,Fe})\text{CO}_3$ show different spectroscopic signatures. The main peak is broader and slightly shifted to higher energy (290.47 eV in Fe-Mag-II and 290.67 eV in Sid-II), and a second peak is observed at 287.35 eV in both compositions (Boulard et al., 2012). These spectroscopic signatures are interpreted as a fingerprint of CO_4 groups, and the slight energy shift of the main peak between the two compositions may reflect different degrees of polymerization of CO_4 groups. Fe content in the $(\text{Mg,Fe})\text{CO}_3$ solid solution likely affects polymerization of CO_4 groups. While isolated $(\text{CO}_4)^{4-}$ tetrahedra are reported in pure Fe composition, high-pressure polymorphs of Mg-rich carbonates are based on polymerized CO_4 groups, i.e. $(\text{C}_3\text{O}_9)^{6-}$ or $(\text{C}_4\text{O}_{13})^{10-}$ chains (Arapan et al., 2007; Boulard et al., 2011; Cerantola et al., 2017; Isshiki et al., 2004; Merlini et al., 2015; Oganov et al., 2008; Panero & Kabbes, 2008).

11.3.2. Self-Redox Reactions in Fe^{2+} -Bearing Carbonates

Another particularity of the crystal chemistry of Fe-bearing high-pressure structures is the preferential association of the CO_4 tetrahedral groups with trivalent iron. Incorporation of trivalent iron or of mixed 3+/2+ valences with high Fe^{3+} contents in these phases was inferred from the stoichiometries (Boulard et al. 2011, 2012; Cerantola et al., 2017; Merlini et al., 2015). Fe $L_{2,3}$ -edges spectra collected ex situ by EELS or scanning transmission X-ray microscopy on the recovered samples from Sid-II or Fe-Mag-II confirmed high Fe^{3+} contents in the products of transformation at high pressure (Boulard et al. 2011, 2012). The redox counterpart for Fe^{3+} formation could eventually be the stabilization of Fe^0 as

observed in the disproportionation reaction of bridgmanite (Frost & McCammon, 2008). However, Fe^0 has never been identified in transformation products of ferromagnesite. Starting from exclusively Fe^{2+} -bearing carbonates, formation of Fe^{3+} is instead balanced by partial reduction of carbon-bearing molecular groups (CO_3^{2-} or CO_2) (Table 11.2). We call this a self-redox process, since Fe^{2+} and CO_3^{2-} initially present in the low-pressure compound react with each other to yield Fe^{3+} and reduced carbon species (C or CO). Diamond coexisting with high-pressure transformation products of Fe^{2+} -bearing carbonates or Fe^{2+} -bearing oxides in presence of CO_2 was reported by Boulard et al. (2011, 2012). Coexisting Fe^{3+} -bearing iron oxides have also been reported, such as magnetite or hematite and their associated high-pressure structures (Boulard et al., 2011, 2012; Cerantola et al., 2017), as well as newly described iron oxides Fe_5O_7 (Cerantola et al., 2017) and $\text{Fe}_{13}\text{O}_{19}$ (Merlini et al., 2015). Decomposition of FeCO_3 into $\text{Fe}_3\text{O}_4 + \text{C}$ was also reported in the stability field of classical CO_3^{2-} -bearing carbonates (<50 GPa) (Boulard et al., 2012; Cerantola et al., 2017). In these low-pressure experiments, only partial decomposition took place, as carbonate remained present even after heating up to one hour. The possible existence of a thermodynamic boundary of siderite decomposition remains to be further investigated. Overall, current available data suggest that the stability of high-pressure phases containing CO_4 groups enhances the disproportionation of Fe^{2+} -bearing carbonates into Fe^{3+} -bearing phases and reduced carbon species such as diamond.

11.4. CONCLUSIONS AND OUTLOOKS

Ferromagnesite $(\text{Mg,Fe})\text{CO}_3$, or close stoichiometries containing oxidized carbon species, are very stable under extreme P-T conditions. The phase diagram of the Mg-Fe-C-O system is very rich and yields several compounds containing CO_4 groups.

Transformation from CO_3 to CO_4 groups may take place at pressure as low as 40 GPa for Fe-rich compositions, and 80 GPa for Mg-rich compositions. As SiO_4

groups in silicates, CO₄ groups may be isolated or polymerized. Impacting the thermodynamic and physical properties of carbonates and associated melts, this new carbon environment may have significant implications on carbon reservoirs and fluxes.

Fe-rich compositions of carbonate are favored at pressure above 40 GPa due to the Fe²⁺ spin transition. The observed systematic presence of trivalent iron in the Fe-rich CO₄-bearing high-pressure structures suggests that other compositions could be stabilized, such as aluminum-rich compositions that do not exist at ambient conditions (Merlini et al., 2015).

These newly described high-pressure structures represent potential oxidized carbon carriers into the lowermost mantle. Whether these phases remain stable in subducting slabs or in regular mantle lithologies is still uncertain. In a recent study, Boulard et al. (2018) reported that the deep carbon and hydrogen cycles may be more interconnected than previously thought, as Fe₄C₃O₁₂ replaces pyrite-structured FeO₂H_x in presence of CO₂, providing a new mechanism for hydrogen release as H₂O within the deep mantle. However, ferromagnesite and the associated high-pressure structures are sensitive to redox breakdown (Dorfman et al., 2018; Rohrbach & Schmidt, 2011; Stagno et al., 2011). Ferromagnesite reacts with metallic iron and nickel in the mantle to form either diamond or carbide, depending on the availability of metal. If this is the case, calcite, which is less sensitive to redox breakdown, could be revived as an interesting oxidized carbon carrier in the deep mantle. More oxidizing conditions like those prevailing in subducting slabs may still stabilize ferromagnesite and related stoichiometries. The redox stabilities of calcite, ferromagnesite, and of their high-pressure transformation products remain to be extensively tested as a function of T, P, and fO₂.

A next step will be to consider the Fe-Mg-C-O high-pressure phase diagram in the context of a silicate-rich lithology. Recent studies on CaCO₃ and MgCO₃ in the presence of an excess of SiO₂ or MgSiO₃ show that CaCO₃ is likely to undergo decomposition into CO₂ and Ca-perovskite under any slab P-T conditions, while MgCO₃ may be preserved under very cold slab P-T conditions (Kakizawa et al., 2015; Maeda et al., 2017; Seto et al., 2008; Takafuji et al., 2006; Z. Zhang et al., 2018). However, none of these studies have considered iron-rich compositions, which deserve special attention due to the effect of the iron spin transition and of self-redox processes with oxidized carbon species. There is increasing evidence that such self-redox processes might be significant. For example, self-redox reaction of ferromagnesite was recently observed in a natural sample of shocked carbonate at the Xiuyan impact crater (Chen et al., 2018). Whether it is related to impact-induced formation of CO₄ groups or not will deserve further

studies. Self-redox processes might also provide relevant explanation for some of the carbonate inclusions in deep diamonds (e.g. Boulard et al., 2011; Brenker et al., 2007; Kaminsky et al., 2012).

ACKNOWLEDGMENTS

E. Boulard acknowledges DCO support during her postdoctoral work. G. Fiquet has received funding from the European Research Council (ERC) under the European Union's Horizon 2020 Research and Innovation Program (grant agreement 670787).

REFERENCES

- Arapan, S., Souza de Almeida, J., & Ahuja, R. (2007). Formation of sp³ hybridized bonds and stability of CaCO₃ at very high pressure. *Physical Review Letters*, 98, 268501. <https://doi.org/10.1103/PhysRevLett.98.268501>
- Biellmann, C., Gillet, P., Guyot, F., Peyronneau, J., & Reynard, B. (1993). Experimental evidence for carbonate stability in the Earth's lower mantle. *Earth and Planetary Science Letters*, 118(1–4), 31–41. [https://doi.org/10.1016/0012-821X\(93\)90157-5](https://doi.org/10.1016/0012-821X(93)90157-5)
- Boulard, E., Gloter, A., Corgne, A., Antonangeli, D., Auzende, A., Perrillat, J.-P., et al. (2011). New host for carbon in the deep Earth. *Proceedings of the National Academy of Sciences of the United States of America*, 108(13), 5184–5187. <https://doi.org/10.1073/pnas.1016934108>
- Boulard, E., Guyot, F., Menguy, N., Corgne, A., Auzende, A., Perrillat, J., & Fiquet, G. (2018). CO₂-induced destabilization of pyrite-structured FeO₂H_x in the lower mantle. *National Science Review*, 5(6), 870–877. <https://doi.org/10.1093/nsr/nwy032>
- Boulard, E., Menguy, N., Auzende, a.-L., Benzerara, K., Bureau, H., Antonangeli, D., et al. (2012). Experimental investigation of the stability of Fe-rich carbonates in the lower mantle. *Journal of Geophysical Research*, 117(B2), B02208. <https://doi.org/10.1029/2011JB008733>
- Boulard, E., Pan, D., Galli, G., Liu, Z., & Mao, W. L. (2015). Tetrahedrally coordinated carbonates in Earth's lower mantle. *Nature Communications*, 6, 6311. <https://doi.org/10.1038/ncomms7311>
- Brenker, F. E., Vollmer, C., Vincze, L., Vekemans, B., Szymanski, A., Janssens, K., et al. (2007). Carbonates from the lower part of transition zone or even the lower mantle. *Earth and Planetary Science Letters*, 260(1–2), 1–9. <https://doi.org/10.1016/j.epsl.2007.02.038>
- Cerantola, V., Bykova, E., Kuppenko, I., Merlini, M., Ismailova, L., McCammon, C., et al. (2017). Stability of iron-bearing carbonates in the deep Earth's interior. *Nature Communications*, 8(May), 15960. <https://doi.org/10.1038/ncomms15960>
- Cerantola, V., Mccammon, C., Kuppenko, I., Kantor, I., Marini, C., Wilke, M., et al. (2015). High-pressure spectroscopic study of siderite (FeCO₃) with a focus on spin crossover. *American Mineralogist*, 100, 2670–2681.

- Chen, M., Shu, J., Xie, X., Tan, D., & Mao, H. (2018). Natural diamond formation by self-redox of ferromagnesian carbonate. *Proceedings of the National Academy of Sciences*, *115*(11), 2676–2680. <https://doi.org/10.1073/pnas.1720619115>
- Dorfman, S. M., Badro, J., Nabiei, F., Prakapenka, V. B., Cantoni, M., & Gillet, P. (2018). Carbonate stability in the reduced lower mantle. *Earth and Planetary Science Letters*, *489*, 84–91. <https://doi.org/10.1016/j.epsl.2018.02.035>
- Dorogokupets, P. I. (2007). Equation of state of magnesite for the conditions of the Earth's lower mantle. *Geochemistry International*, *45*(6), 561–568. <https://doi.org/10.1134/S0016702907060043>
- Egerton, R. F. (1996). *Electron energy-loss spectroscopy in the electron microscope* (2nd ed.). New York: Press Plenum.
- Fiquet, G., Guyot, F., Kunz, M., Matas, J., Andrault, D., & Hanfland, M. (2002). Structural refinements of magnesite at very high pressure. *American Mineralogist*, *87*, 1261–1265. <https://doi.org/10.2138/am-2002-8-927>
- Frost, D. J., & McCammon, C. A. (2008). The redox state of Earth's mantle. *Annual Review of Earth and Planetary Sciences*, *36*, 389–420. <https://doi.org/10.1146/annurev.earth.36.031207.124322>
- Gillet, P. (1993). Stability of magnesite (MgCO₃) at mantle pressure and temperature conditions: A Raman spectroscopic study. *American Mineralogist*, *78*, 1328–1331.
- Graf, D. L. (1961). Crystallographic tables for the rhombohedral carbonates. *American Mineralogist*, *46*, 1283–1316.
- Hofer, F., & Golob, P. (1987). New examples for near-edge fine structures in electron energy loss spectroscopy. *Ultramicroscopy*, *21*, 379–383.
- Irifune, T., Isshiki, M., & Sakamoto, S. (2005). Transmission electron microscope observation of the high-pressure form of magnesite retrieved from laser heated diamond anvil cell. *Earth and Planetary Science Letters*, *239*(1–2), 98–105. <https://doi.org/10.1016/j.epsl.2005.05.043>
- Isshiki, M., Irifune, T., Hirose, K., Ono, S., Ohishi, Y., Watanuld, T., et al. (2004). Stability of magnesite and its high-pressure form in the lowermost mantle. *Nature*, *427*(January), 60–63. <https://doi.org/10.1029/2000C000736>
- Kakizawa, S., Inoue, T., Suenami, H., & Kikegawa, T. (2015). Decarbonation and melting in MgCO₃-SiO₂ system at high temperature and high pressure. *Journal of Mineralogical and Petrological Sciences*, *110*(4), 179–188. <https://doi.org/10.2465/jmps.150124>
- Kaminsky, F. (2012). Mineralogy of the lower mantle: A review of “super-deep” mineral inclusions in diamond. *Earth-Science Reviews*, *110*, 127–147. <https://doi.org/10.1016/j.earscirev.2011.10.005>
- Katsura, T., Tsuchida, Y., Ito, E., Yagi, T., Utsumi, W., & Akimoto, S. (1991). Stability of magnesite under the lower mantle conditions. *Proceedings of the Japan Academy. Ser. B: Physical and Biological Sciences*, *67*(4), 57–60. <https://doi.org/10.2183/pjab.67.57>
- Kelemen, P. B., & Manning, C. E. (2015). Reevaluating carbon fluxes in subduction zones: What goes down, mostly comes up. *Proceedings of the National Academy of Sciences*, *112*(30), E3997–E4006. <https://doi.org/10.1073/pnas.1507889112>
- Kushiro, I., Satake, H., Akimoto, S. (1975). Carbonate-silicate reactions at high pressures and possible presence of dolomite and magnesite in the upper mantle. *Earth and Planetary Science Letters*, *28*, 116–120. [https://doi.org/10.1016/0012-821X\(75\)90218-6](https://doi.org/10.1016/0012-821X(75)90218-6)
- Lavina, B., Dera, P., Downs, R., Yang, W., Sinogeikin, S., Meng, Y., et al. (2010). Structure of siderite FeCO₃ to 56 GPa and hysteresis of its spin-pairing transition. *Physical Review B*, *82*(6), 1–7. <https://doi.org/10.1103/PhysRevB.82.064110>
- Liang, W., Yin, Y., Li, Z., Li, R., Li, L., He, Y., et al. (2018). Single crystal growth, crystalline structure investigation and high-pressure behavior of impurity-free siderite (FeCO₃). *Physics and Chemistry of Minerals*, *45*(9), 831–842. <https://doi.org/10.1007/s00269-018-0965-y>
- Liu, J., Lin, J. F., Mao, Z., & Prakapenka, V. B. (2014). Thermal equation of state and spin transition of magnesiosiderite at high pressure and temperature. *American Mineralogist*, *99*(1), 84–93. <https://doi.org/10.2138/am.2014.4553>
- Liu, J., Lin, J.-F., & Prakapenka, V. B. (2015). High-pressure orthorhombic ferromagnesite as a potential deep-mantle carbon carrier. *Scientific Reports*, *5*, 7640. <https://doi.org/10.1038/srep07640>
- Lin, J. F., Liu, J., Jacobs, C., & Prakapenka, V. B. (2012). Vibrational and elastic properties of ferromagnesite across the electronic spin-pairing transition of iron. *American Mineralogist*, *97*(4), 583–591. <https://doi.org/10.2138/am.2012.3961>
- Lobanov, S. S., Dong, X., Martirosyan, N. S., Samtsevich, A. I., Stevanovic, V., Gavryushkin, P. N., et al. (2017). Raman spectroscopy and x-ray diffraction of sp³-CaCO₃ at lower mantle pressures. *Physical Review B*, *96*, 104101. <https://doi.org/10.1103/PhysRevB.96.104101>
- Lobanov, S. S., Goncharov, A. F., & Litasov, K. D. (2015). Optical properties of siderite (FeCO₃) across the spin transition: Crossover to iron-rich carbonates in the lower mantle. *American Mineralogist*, *100*(5–6), 1059–1064. <https://doi.org/10.2138/am-2015-5053>
- Maeda, F., Ohtani, E., Kamada, S., Sakamaki, T., Hirao, N., & Ohishi, Y. (2017). Diamond formation in the deep lower mantle: A high-pressure reaction of MgCO₃ and SiO₂. *Scientific Reports*, *7*(January), 40602. <https://doi.org/10.1038/srep40602>
- Mao, W. L., & Boulard, E. (2013). Nanoprobes for deep carbon. *Reviews in Mineralogy and Geochemistry*, *75*(1), 423–448. <https://doi.org/10.2138/rmg.2013.75.13>
- Martirosyan, N. S., Litasov, K. D., Shatskiy, A. F., & Ohtani, E. (2015). Reactions of iron with calcium carbonate at 6 GPa and 1273–1873 K: Implications for carbonate reduction in the deep mantle. *Russian Geology and Geophysics*, *56*(9), 1322–1331. <https://doi.org/10.1016/j.rgg.2015.08.008>
- Mattila, a, Pyllkkänen, T., Rueff, J.-P., Huotari, S., Vankó, G., Hanfland, M., et al. (2007). Pressure induced magnetic transition in siderite FeCO₃ studied by x-ray emission spectroscopy. *Journal of Physics: Condensed Matter*, *19*(38), 386206. <https://doi.org/10.1088/0953-8984/19/38/386206>
- Merlini, M., Hanfland, M., Salamat, A., Petitgirard, S., & Müller, H. (2015). The crystal structures of Mg₂Fe₂C₄O₁₃ with tetrahedrally coordinated carbon, and Fe₁₃O₁₉, synthesized at deep mantle conditions. *American Mineralogist*, *100*, 2001–2004. <https://doi.org/10.1524/zkri.219.10.621.50817>
- Oganov, A. R., Glass, C. W., & Ono, S. (2006). High-pressure phases of CaCO₃: Crystal structure prediction and

- experiment. *Earth and Planetary Science Letters*, 241(1–2), 95–103. <https://doi.org/10.1016/j.epsl.2005.10.014>
- Oganov, A. R., Ono, S., Ma, Y., Glass, C. W., & Garcia, A. (2008). Novel high-pressure structures of MgCO₃, CaCO₃ and CO₂ and their role in Earth's lower mantle. *Earth and Planetary Science Letters*, 273, 38–47. <https://doi.org/10.1016/j.epsl.2008.06.005>
- Ono, S. (2008). Experimental constraints on the temperature profile in the lower mantle. *Physics of the Earth and Planetary Interiors*, 170, 267–273. [doi:10.1016/j.pepi.2008.06.033](https://doi.org/10.1016/j.pepi.2008.06.033)
- Panero, W. R., & Kabbes, J. E. (2008). Mantle-wide sequestration of carbon in silicates and the structure of magnesite II. *Geophysical Research Letters*, 35(14), 1–5. <https://doi.org/10.1029/2008GL034442>
- Rohrbach, A., & Schmidt, M. W. (2011). Redox freezing and melting in the Earth's deep mantle resulting from carbon-iron redox coupling. *Nature*, 472(7342), 209–12. <https://doi.org/10.1038/nature09899>
- Santillán, J., Catalli, K., & Williams, Q. (2005). An infrared study of carbon-oxygen bonding in magnesite to 60 GPa. *American Mineralogist*, 90(10), 1669–1673. <https://doi.org/10.2138/am.2005.1703>
- Santillán, J., & Williams, Q. (2004). A high-pressure infrared and X-ray study of FeCO₃ and MnCO₃: Comparison with CaMg(CO₃)₂-dolomite. *Physics of the Earth and Planetary Interiors*, 143(1–2), 291–304. <https://doi.org/10.1016/j.pepi.2003.06.007>
- Scott, H. P., Doczy, V. M., Frank, M. R., Hasan, M., Lin, J.-F., & Yang, J. (2013). Magnesite formation from MgO and CO₂ at the pressures and temperatures of Earth's mantle. *American Mineralogist*, 98(7), 1211–1218. <https://doi.org/10.2138/am.2013.4260>
- Seto, Y., Hamane, D., Nagai, T., & Fujino, K. (2008). Fate of carbonates within oceanic plates subducted to the lower mantle, and a possible mechanism of diamond formation. *Physics and Chemistry of Minerals*, 35, 223–229. <https://doi.org/10.1007/s00269-008-0215-9>
- Skorodumova, N. V. (2005). Stability of the MgCO₃ structures under lower mantle conditions. *American Mineralogist*, 90, 1008–1011. <https://doi.org/10.2138/am.2005.1685>
- Solopova, N. A., Dubrovinsky, L., Spivak, A. V., Litvin, Y. A., & Dubrovinskaia, N. (2015). Melting and decomposition of MgCO₃ at pressures up to 84 GPa. *Physics and Chemistry of Minerals*, 42(1), 73–81. <https://doi.org/10.1007/s00269-014-0701-1>
- Stagno, V., Tange, Y., Miyajima, N., Mccammon, C. A., Irifune, T., & Frost, D. J. (2011). The stability of magnesite in the transition zone and the lower mantle as function of oxygen fugacity. *Geophysical Research Letters*, 38, L19309. <https://doi.org/10.1029/2011GL049560>
- Syracuse, E. M., Van Keken, P. E., Abers, G. A., Suetsugu, D., Editor, G., Bina, C., et al. (2010). The global range of subduction zone thermal models. *Physics of the Earth and Planetary Interiors*. <https://doi.org/10.1016/j.pepi.2010.02.004>
- Takafuji, N., Fujino, K., Nagai, T., Seto, Y., & Hamane, D. (2006). Decarbonation reaction of magnesite in subducting slabs at the lower mantle. *Physics and Chemistry of Minerals*, 33(10), 651–654. <https://doi.org/10.1007/s00269-006-0119-5>
- Tao, R., Fei, Y., & Zhang, L. (2013). Experimental determination of siderite stability at high pressure. *American Mineralogist*, 98, 1565–1572. <https://doi.org/10.2138/am.2013.4351>
- Tateno, S., Hirose, K., Ohishi, Y., & Tatsumi, Y. (2010). The structure of iron in Earth's inner core. *Science*, 330, 359–361. <https://doi.org/10.1126/science.1194662>
- Thomson, A. R., Walter, M. J., Kohn, S. C., & Brooker, R. A. (2016). Slab melting as a barrier to deep carbon subduction. *Nature*, 529(7584), 76–79. <https://doi.org/10.1038/nature16174>
- Wang, A., Pasteris, J. D., Meyer, H. O. A., & Dele-duboi, M. L. (1996). Magnesite-bearing inclusion assemblage in natural diamond, 141, 293–306.
- Weis, C., Sternemann, C., Cerantola, V., Sahle, C. J., Spiekermann, G., Harder, M., et al. (2017). Pressure driven spin transition in siderite and magnesiosiderite single crystals. *Scientific Reports*, 7(1), 1–10. <https://doi.org/10.1038/s41598-017-16733-3>
- Wood, B. J., Pawley, A., & Frost, D. R. (1996). Water and carbon in the Earth's mantle. *Philosophical Transactions of the Royal Society of London*, 354, 1495–1511.
- Zhang, J., Martinez, I., Guyot, F., & Reeder, R. J. (1998). Effects of Mg-Fe 2+ substitution in calcite-structure carbonates: Thermoelastic properties. *American Mineralogist*, 83, 280–287.
- Zhang, Z., Mao, Z., Liu, X., Zhang, Y., & Brodholt, J. (2018). Stability and reactions of CaCO₃ polymorphs in the Earth's deep mantle. *Journal of Geophysical Research: Solid Earth*, 123(8), 6491–6500. <https://doi.org/10.1029/2018JB015654>
- Zhou, D., Metzler, R. A., Tyliszczak, T., Guo, J., Abrecht, M., Coppersmith, S. N., & Gilbert, P.U.P.A. (2008). Assignment of polarization-dependent peaks in carbon K-edge spectra from biogenic and geologic aragonite. *Journal of Physical Chemistry B*, 112(41), 13128–13135. <https://doi.org/10.1021/jp803176z>